Density functional theory study of the optoelectronic properties of new D′-D-π-A type organic dyes for dye-sensitized solar cells

M. Yanadhi Rao[a], N. Murali Krishna[b], G.Ravi Kumar[c], Mannam SubbaRao[d*]

[a]Department of Chemistry, SCIM Government Degree College, Tanuku, W.G. Dist., A.P., India.
[b]Department of Chemistry, V.R. Siddhartha Enginnering College, Kanuru, Vijayawada-520 007, A.P., India.
[c]Department of Chemistry, Government Degree College(Autonomous), Siddipet- 502 103, T.S., India
[d]Department of Chemistry, Acharya Nagarjuna University, Guntur-522 510, A.P., India.

Abstract

Density functional theory and time-dependent approaches are used for the theoretical investigation of a new class of novel carbazole-based D′-D-π-Atype dyes. For all the dyes under study, the primary electron donor is the carbazole moiety, with 4H-cyclopenta[c]thiophene acting as a π-bridge and cyanoacrylic acid serving as the electron acceptor. The effect of the terminal electron donor on the optoelectronics properties is examined for the dyes in their isolated condition and the acetonitrile solvent. Their electronic and structural characteristics, as well as their absorption spectra, are analysed and explained. All of the dyes showed good optoelectronic capabilities, according to the theoretical findings. Based on its red-shifted absorption spectrum, smaller energy gap, lowest total value, and higher $G^{injec}t$ and G^{Reg}, D5 with methyl substituted thiopheneas the terminal electron donor moiety, in particular, has had the potential to be used as a sensitizer for nanocrystalline TiO2 solar cells.

Keywords:9-vinyl-9H-carbazole, D′–D–π–A structure, optoelectronic properties,HOMO-LUMO, DFT, and TD-DFT methods

1. Introduction

Although fossil fuels continue to be the most commonly used energy source worldwide, there have been concerns about whether the available sources will soon exhaust themselves [1]. In addition, concerns regarding the pervasiveness of global warming brought on by energy use have also been widely expressed [2]. Renewable energy sources, as opposed to fossil fuels, have several benefits: they replenish themselves organically, create little secondarywaste, cut down on greenhouse gas emissions, and support sustainability [3,4]. Bioenergy, direct solar energy, geothermal energy, hydropower, wind, and ocean energy (tide and wave) are some of these sources [4]. Solar collectors and photovoltaic (PV) systems are direct solar energy sources. Both systems use the photoelectric effect to produce energy.Due to their hole transportation and charge carrier mobility, the first-generation PV systems comprised of silicon are still mostly in use [5]. However, it is challenging to deploy silicon-based PV systems due to the difficulty in making silicon solar cells and their high manufacturing costs. Due to these difficulties, a lot of research has lately been done to find inexpensive materials to replace silicon in PV systems. Dye-sensitized solar cells (DSSCs) are one of these materials because of their low cost, simple manufacture, minimal toxicity, and excellent power conversion efficiencies. Furthermore, it has been demonstrated that these cells function in low light [6].

Due to their potential benefits of low cost, simple production, flexibility, and transparency compared to conventional silicon solar cells [7-9], dye-sensitized solar cells (DSSCs) have attracted a lot of interest in the field of materials science over the past 20 years since they were first reported by O'Regan and Grätzel [10]. Due to their photophysical and photochemical characteristics, coordination complexes of ruthenium, which are present in these devices and provide DSSCs with extraordinarily high photoelectric conversion efficiencies, have attracted a lot of attention. A cobalt electrolyte and ruthenium-based dyes have been used in devices with power conversion efficiency above 12% [11].

However, because these dyes contain the noble metal ruthenium, which is pricey and necessitates a challenging purification process, they are seldom suitable for use in lucrative and ecologically responsible photovoltaic systems [12]. Because of their simple synthesis, high molar extinction coefficient, tenable absorption spectrum response from the visible to infrared area, as well as their ecologically friendly and low-cost production procedures, organic dyes have been the focus of intensive research efforts [13, 14]. In recent years, significant improvements in conversion efficiency have been made using this type of dye, with levels ranging from 7.1% in 1991 to 13% in 2014 [15].Due to its efficient photoinduced intramolecular charge-transfer properties, donor-linker-acceptor (D-A) dipolar structures are designed into most organic dyes [16].

The development of such organic dyes using the donor groups carbazole [17], triphenylamine [18–20], indole, and indoline [21–24], has led to reports of DSSCs with exceptional effectiveness. Among the aromatic heterocyclic compounds, carbazole and its derivatives are essential groups because of their potent capacity to donate electrons [25]. These units have been frequently used as a functional building block in the D-A architecture to create organic photoconductors and nonlinear optical materials due to their unique electrochemical and optical properties [26, 27], excellent structural stability, and coplanarity with the donor and acceptor units. The carbazole molecule's crowded configuration also helps prevent intramolecular aggregation [18].Due to the cyanide group's strong electron attraction capabilities, cyanoacrylic acid is frequently utilized as an electron acceptor moiety. The electron donor and acceptor are connected by a -bridge, which spreads the electron density and makes charge separation during excitation possible. A -bridge has the benefits of expanding the maximum absorption peak, tuning the higher occupied (HOMO) and lowest unoccupied (LUMO) levels, and lowering charge recombination. Thiophene and its derivatives, particularly bithiophene, have better charge-transfer characteristics among the substances typically employed as the -bridge, making them the potential -bridge moieties for dye sensitizers with a smaller energy gap and improved photocurrent [28]. The main drawback of these organic dyes is that they may clump on the semiconductor surface, which lowers the photoconversion efficiency [29]. Researchers have devised plans to create highly efficient sensitizers to remedy this. One of the most crucial strategies is altering organic dyes by changing their essential components. By adding different terminal electron donors to create sensitizers that can improve the optical and electrophysical properties of DSSCs, the current study makes an intriguing advancement in this area.

In this study, we investigate several D′-D-A-type organic dyes with cyanoacrylic acid acting as the electron acceptor, 4H-cyclopenta[c]thiophene as the significant electron donor, and 9-vinyl-9H-carbazole (D) as the primary electron donor (A). Eight chemical colours, designated S1 through S8, are produced when different substituted thiophene donors (D′), or substituted

thiophene, are substituted for carbazole. The compounds' structural, optical, and electrochemical characteristics are examined (Fig.1)

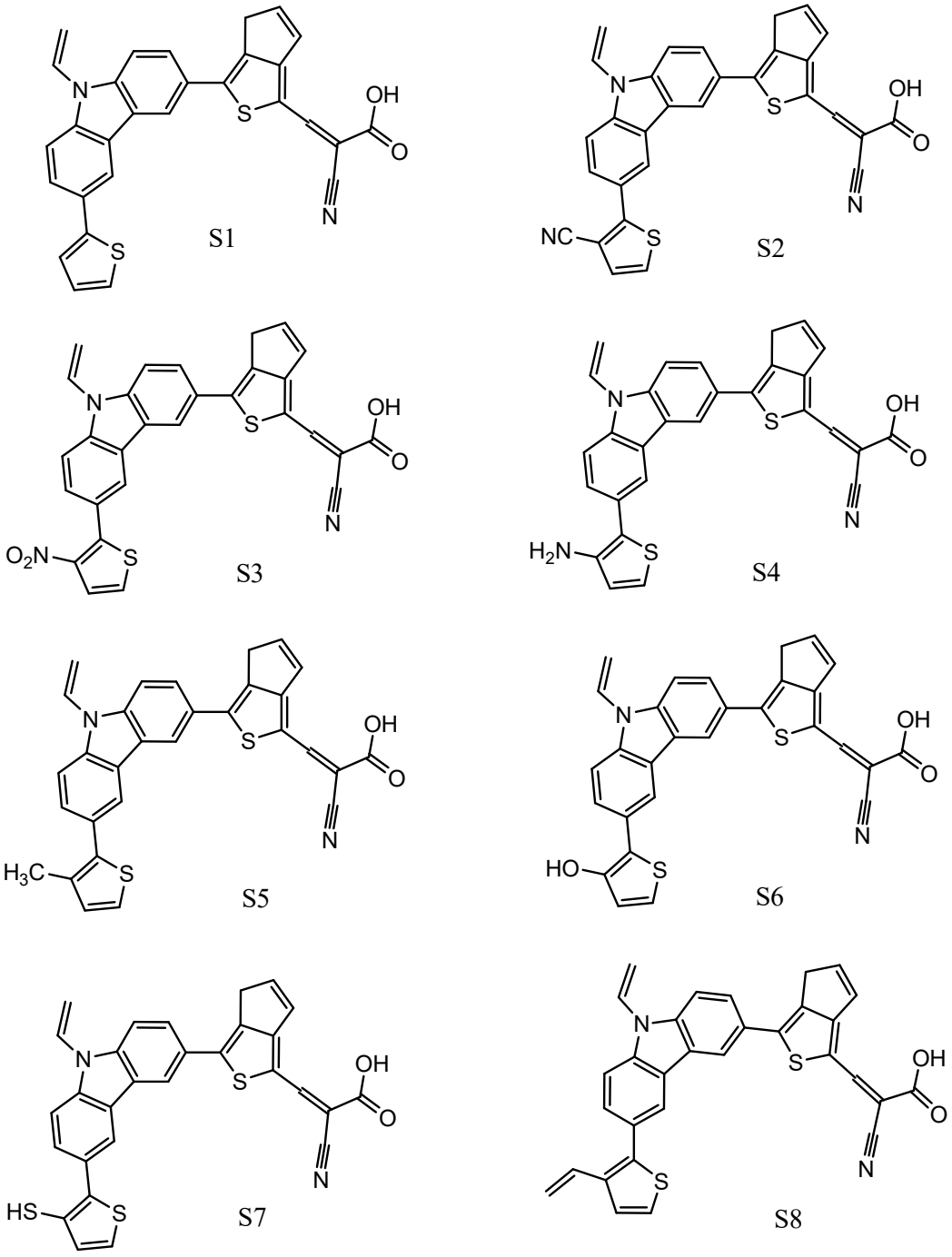

Figure 1. Chemical structure for the D'-D-π-A sensitizers

2. Methodology

Using the Gaussian 09 software, all computations are performed in an isolated setting with chloroform as the solvent [30]. Density functional theory (DFT) and the hybrid functional B3LYP are used to optimize the ground-state geometry [31] fully, and the B3LYP and the identical 6-311G++ basis set are used to calculate the unpaired electron spin densities of radical cations [32,33]. To simulate the ultraviolet-visible (UV-Vis) absorption spectra in acetonitrile solvent with the polarizable continuum model of solvation (PCM) [34-36], excited-state calculations are also carried out using time-dependent (TD) DFT with B3LYP [34] using the same basis set.The GAUSSVIEW program [37] and Gabedit software [38] simulate the plots of the optical absorption spectra and the graphical display of the estimated optical absorption spectra. The electronic density distribution utilized to explain the optical and electronic characteristics of the sensitizers is displayed using the energy evels of the extracted molecular orbitals. In the DSSC, electron injection and dye regeneration are accomplished using the semiconductor TiO2 and the iodine/iodide redox pair, respectively. The total reorganization energy (total) of the dyes is determined by optimizing their cationic and anionic states at the B3LYP/6-31G++ level.

3 Results and discussion

3.1. Optimized Geometry structure

We investigate several carbazole-based organic dyes, S1 explicitly through S8, to identify a chemical structure with advantageous optoelectronic characteristics for DSSC application. The precision of a molecule's optimized structure significantly impacts the projected property. Before any structure reaches its most minor energy configuration or the optimized structure, several optimization processes are necessary (Figure 2).By using frequency calculations, the optimized structures were verified as minima or transition state structures. Higher-order saddle points are given to structures with two or more imaginary frequencies because any structure with one imaginary frequency (i.e., negative vibrational frequency) is denoted by a transition state. A structure that has achieved its minimum energy should not have a negative frequency, indicating that it is fully optimized.

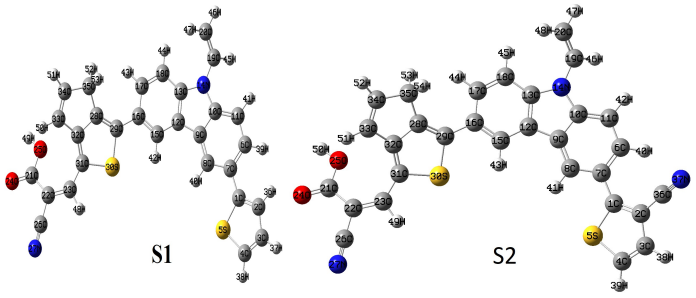

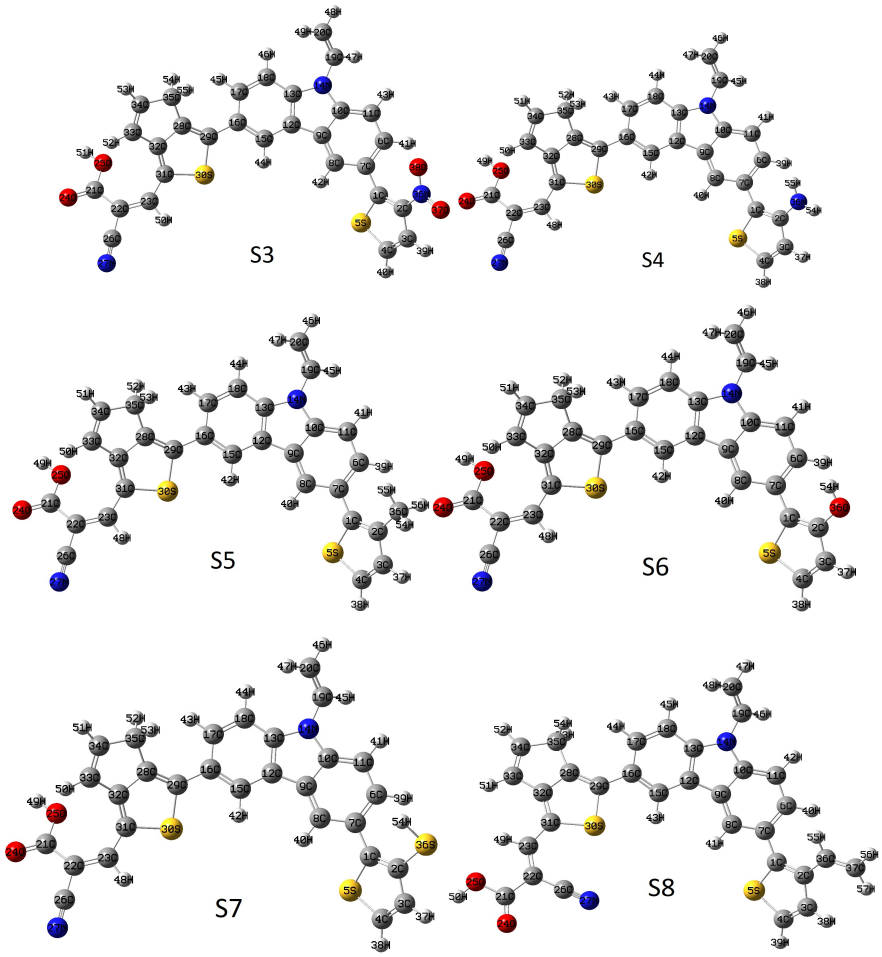

Figure 2: Optimization structures in gas phase calculated by DFT/6-311G++ basis set.

3.2 Molecular orbital calculations

Fig. 3 shows the HOMO and LUMO electron density patterns of the investigated dyes. While the LUMO exhibits bonding between two neighbouring fragments, the HOMO exhibits antibonding. In Fig. 3, we can see that the carbazole-containing -orbitals of the donor, the terminal electron donor, and the -linker unit are the primary sources of the electron density of the HOMO of all the dyes under study. The cyanoacrylic acid unit and the -linker are where the LUMO's electron density is most strongly localized for all investigated compounds. For the dyes S2, S3, S4, S6, and D5, the electronic transition from HOMO to LUMO contributed more than 65%, whereas S1, S5, S7, and S8 contributed about 50%.

As a result, we think that all dyes undergo an electrical shift from the HOMO to the LUMO. When exposed to photons, an excited electron transfers from the donor composed of methyl-indole and carbazole to the cyanoacrylic acid acceptor via the -linker group, resulting in effective charge separation and electron injection, according to the distributions of the HOMO and LUMO electron densities.

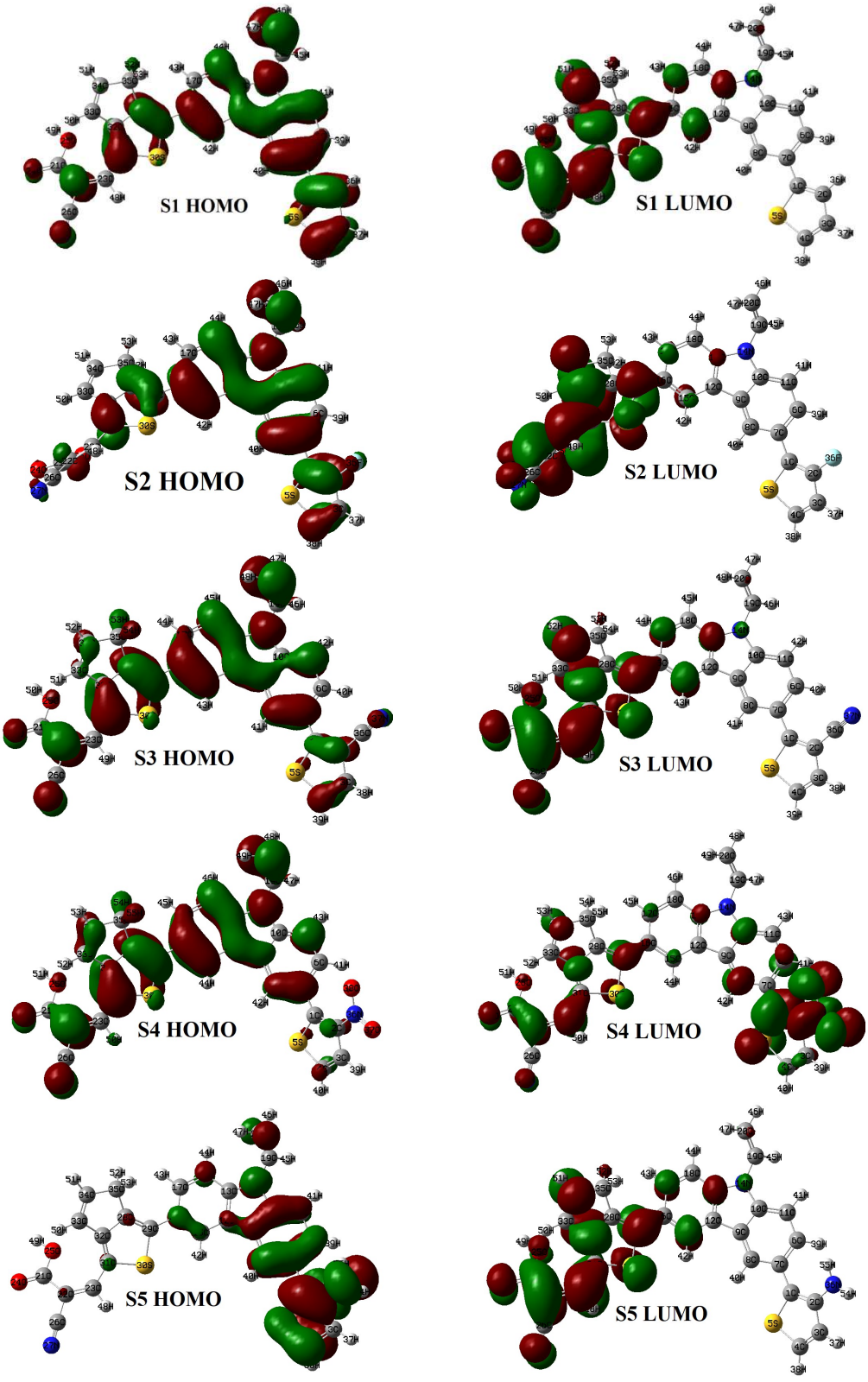
S1 HOMO
S1 LUMO
S2 HOMO
S2 LUMO
S3 HOMO
S3 LUMO
S4 HOMO
S4 LUMO
S5 HOMO
S5 LUMO

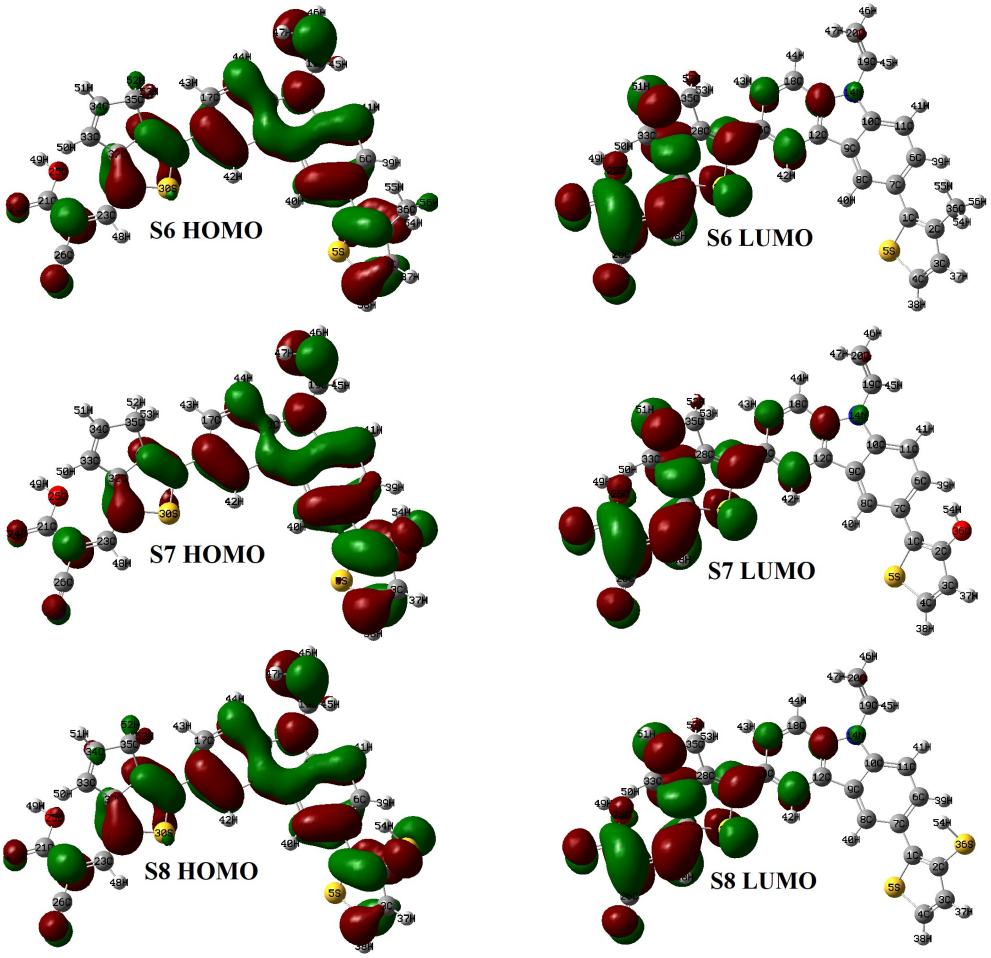

Figure 3: The counter plots of molecular orbitals HOMO and LUMO of studied dyes S1-S9 at B3LYP/6-311G++ level of theory in the gas phase.

3.3 Electronic properties

The quantum-chemical study is carried out by altering the electron donor capability to clarify the impact of the terminal electron donor on the electronic properties of the examined dyes for application in DSSCs. Table 1 lists the findings of this analysis of the border molecular orbital energies (HOMO and LUMO) and the energy gap (Eg) of these dyes. In contrast, Figs. 4 and 5 depict energy level diagrams for the gas and solvent phases, illustrating the HOMO and LUMO.The LUMO provides a thermodynamic driving force for effective electron injection because it is located above the conduction band of TiO2 (around 4.00 eV in vacuum). The examined dyes quickly regenerate while the HOMO is below the iodide redox potential (4.80 eV in vacuum) [39,40], which causes charge recombination between the oxidized dye and photoinjected electrons in the TiO2 semiconductor [41].

Table 1 HOMO energy, LUMO energy and Energy gap (Eg) values in eV of the donor monomers obtained by DFT/B3LYP/6-311G level calculations in gas and Acetonitrile

Dye	Gas			Solvent		
	HOMO(eV)	LUMO (eV)	Eg(eV)	HOMO(eV)	LUMO (eV)	Eg(eV)
S1	-5.5325	-2.7935	-2.7391	-5.4482	-2.8577	-2.5905
S2	-5.7644	-2.8879	-2.8765	-5.5998	-2.9053	-2.6944
S3	-5.8191	-2.9660	-2.8531	-5.6474	-3.0846	-2.5627
S4	-5.0602	-2.7505	-2.3097	-5.0191	-2.8849	-2.1342
S5	-5.5461	-2.7859	-2.7603	-5.4661	-2.8906	-2.5755
S6	-5.5554	-2.8367	-2.7187	-5.4457	-2.8961	-2.5497
S7	-5.6498	-2.8392	-2.8106	-5.5312	-2.8972	-2.6340
S8	-5.4569	-2.7325	-2.7244	-5.4827	-2.8838	-2.5989

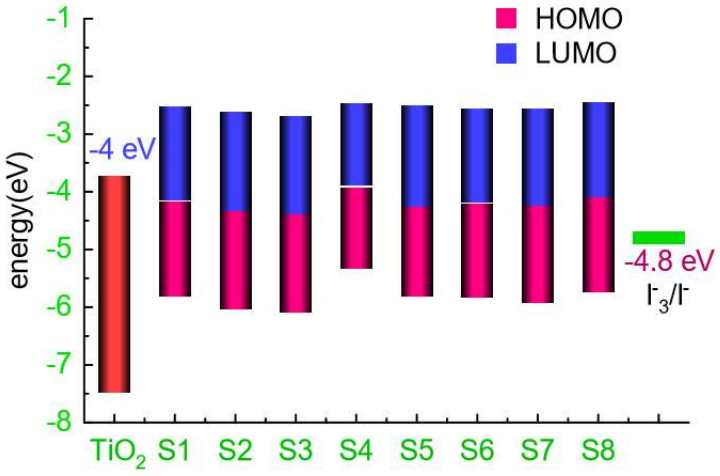

Figure 4. Energy level plot of the designed compounds S1 to S9in gas phase.

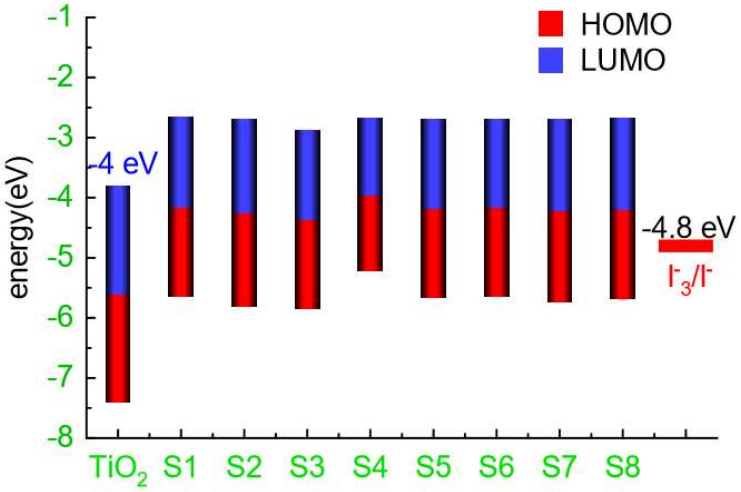

Figure 5. Energy level plot of the designed compounds S1 to S9in gas phase.

Based on Table 1, observe that the HOMO energies decline in the following order: S3<S2<S7<S6<S5<S8<S1<S4, whereas the LUMO energies were identical for all compounds in the gas and solvent phases except S3. This demonstrates that the considerable influence of the terminal electron donor on the examined compound's HOMO affects the order relative to the energy gap. Additionally, we point out that S4 has a smaller gap than the other dyes under study due to its high HOMO energy. Therefore, unlike the dye S4, this dye is not too occupied, possibly due to the more substantial terminal donor and higher conjugation between the donors and conjugated -system.

4 Photovoltaic Parameters

A DSSC's short-circuit photocurrent density (J_{SC}), open-circuit potential (V_{OC}), fill factor (FF), and incident light intensity are all strongly correlated with its power conversion efficiency (). (Pinc). This can be said in the following way [42]:

$$\eta=FF\frac{J_{SC}V_{OC}}{P_{inc}} \quad (1)$$

Where P_{inc} is the intensity of the incident light, FF is the fill factor, V_{oc} is the open circuit voltage, J_{sc} is the short circuit current density, and The fill factor is calculated using the following equation (2) [43].

$$FF=\frac{I_m\times V_m}{J_{sc}\times V_{oc}} \quad (2)$$

The integral of the product of the light-harvesting efficiency of photons at wavelength, or LHE(λ), the electron injection efficiency φ_{inject} and the charge collecting efficiency $\eta_{collect}$collect can be used to calculate the short-circuit photocurrent density (J_{SC}) [44–46].

$$J_{sc}=e\int LHE(\lambda)\phi_{inj}.\eta_{reg}.\eta_{cc}.I_s(\lambda)d\lambda \quad (3)$$

The dye's reaction to the incident light also plays a role in a DSSC's efficiency. Therefore, the light-harvesting efficiency (LHE) should be as high as possible to enhance the photocurrent response. The LHE is denoted by [47].

$$LHE=1-10^{-f} \quad (4)$$

where f is the dye molecules' oscillator strength. We can infer from Equation (4) that a considerable oscillator strength will result in a high LHE. Another term that expresses the likelihood of electromagnetic radiation absorption by changes in an atom's or molecule's energy level is oscillator strength (f). Tables 2and 5 shows the oscillator strength values for these dyes in the gas and solvent phases, respectively, at the maximum absorption.The light harvesting efficiency is a factor connected with DSSC efficiency and oscillator strength (LHE). These dyes must have a high LHE for the photocurrent response to be as strong as possible. All of these dyes have LHE values that vary from 0.4259 to 0.8204. (Table 2). Due to the slight variation in LHE values, all sensitizers will produce comparable photocurrents.

Table 2: The light harvesting efficiency (LHE),binding energy (Eb) and open-circuit voltage (Voc) calculated using DFT/B3LYP/6-311G++ level of theory.

Dye	LHE		V_{OC} eV		Eb eV	
	gas	sol	gas	sol	gas	sol
S1	0.5398	0.6342	1.2065	1.1423	0.2735	0.3921
S2	0.7360	0.7946	1.1121	1.0947	0.2526	0.2814
S3	0.4259	0.4391	1.034	0.9154	0.3509	0.5824
S4	0.7757	0.8204	1.2495	1.1151	0.2781	0.8533
S5	0.5801	0.6819	1.2141	1.1094	0.5110	0.6413
S6	0.4594	0.6255	1.1633	1.1039	0.2763	0.4537
S7	0.5977	0.7235	1.1608	1.1028	0.2648	0.3514
S8	0.4436	0.6139	1.2675	1.1162	0.2780	0.4374

The electro-optical characteristics and electron-hole pair dissociation potential of the metal-free organic dye affect a DSSC's efficiency. Binding (Coulomb attractive) energy holds the electron to its hole because Coulombic forces exist between electron-hole pairs. The electron-hole pair experiences a strong Coulombic force due to the low dielectric constant of organic molecules, leading to a high binding energy that is inversely proportional to the dissociation energy. The electron leaves its hole as a result of the latter. The relationship between binding energy, band gap energy, and single point excitation energy is given by equation (5):

$$E_b = E_{(LUMO-HOMO)} - E_{(S0-S1)} \quad (5)$$

Where $E_{(LUMO-HOMO)}$ is the band gap energy; $E_{(S1-S0)}$ is the single point excitation energy between the ground and the excited state; and Eb is the binding energy, also known as the estimation of the excitation's dissociation energy (Table 2). An electron must have positive single-point energy to excite it to the LUMO level successfully. Additionally, this sets it apart from its hole [48].

Studying the photovoltaic performance dramatically benefits from calculating the electron injection rate from the dye to the conduction band of the TiO_2 semiconductor and the regeneration of the dye by the electrolyte. The change in free energy (in eV) corresponding to electron injection and regeneration can be calculated using the following equation [49, 50]:

$$\Delta G^{inject} = E_{OX}^{dye*} - E_{CB}^{TiO_2} \quad (6)$$

$$\Delta G^{Reg} = E_{I^-/I^{3-}} - E_{HOMO} \quad (7)$$

where E_{OX}^{dye*} the dye's excited-state oxidation potential energy, the TiO_2 conduction band's reduction potential ($E_{CB}^{TiO_2} = 4.0$ eV), and thenI^-/I_3^-redox potential ($E_{I^-/I^{3-}} = 4.8$ eV) are all equal [49, 51] can be projected to be the following relation[52]

$$E_{OX}^{dye*} = E_{OX}^{dye} - E_{exc} \quad (8)$$

where E_{xec} is the electronic vertical transition energy corresponding to max λ_{max}[52] E_{OX}^{dye}, the dye's oxidative potential energy in its ground statecan be calculated as E_{HOMO}'s negative value [49].

The free injection electron energy $G^{inject}$and Greg are crucial variables when examining how the electronic structure and J_{SC} relate. Fast electron transport requires low G^{inject} and G^{Reg}. Table 3 displays the calculated values for these parameters. The excited electron in the dye can easily escape into the conduction band of TiO_2, supporting the injection phenomena, as shown by the fact that G^{inject} is harmful to all the chosen dyes. Additionally, all the examined dyes had increased G^{injec}t values in the order S4 = 0.86 eV and G^{Reg} = 0.26 eV, resulting in a significant IPCE.

Table 3 The free injection energy (ΔG^{Inject}) free regeneration energy (ΔG^{Reg}), open-circuit voltage (V_{OC}) and binding energy (Eb)calculated at the DFT/ B3LYP/6–311Glevels.

Gas					
Dye	E_{OX}^{dye}	**E_{exc}**	E_{OX}^{dye*}	**ΔG^{Inject}**	**ΔG^{Reg}**
S1	5.5325	2.4656	3.0669	-0.9331	0.7325
S2	5.7644	2.6239	3.1405	-0.8595	0.9644
S3	5.8191	2.5022	3.3169	-0.6831	1.0191
S4	5.0602	2.0316	3.0286	-0.9714	0.2602
S5	5.5461	2.2493	3.2968	-0.7032	0.7461
S6	5.5554	2.4424	3.1130	-0.8870	0.7554
S7	5.6498	2.5458	3.1040	-0.8960	0.8498
S8	5.4569	2.4464	3.0105	-0.9895	0.6569
Solvent					
S1	5.4482	2.2858	3.1624	-0.8376	0.6482
S2	5.5998	2.3939	3.2059	-0.7941	0.7998
S3	5.6474	2.1887	3.4587	-0.5413	0.8474
S4	5.0191	1.887	3.1321	-0.8679	0.2191
S5	5.4661	2.2773	3.1888	-0.8112	0.6661
S6	5.4457	2.2513	3.1944	-0.8056	0.6457
S7	5.5312	2.3367	3.1945	-0.8055	0.7312
S8	5.4827	2.2925	3.1902	-0.8098	0.6827

The difference between the electrolyte's redox potential and the electron's quasi-Fermi level in the conduction band of TiO_2 is measured by the open-circuit voltage (V_{OC}). The rate of charge recombination is slower when the Voc value is high. The main contributors to a photovoltaic cell's Voc are its Lumos and conduction band, both found in the semiconductor TiO_2. This is explained by Eq. (9) and the illustration of Voc in Table 2. [53]:

$$V_{OC} = E_{LUMO} - E_{CB}^{TiO_2} \quad (9)$$

The open-circuit voltage (V_{OC}) and Jsc values also impact the overall efficiency of power conversion. According to Eq. (9), the examined dyes' V_{OC} values range from 0.9 eV to 1.26 eV, showing that they all have higher V_{OC} values than S2 and S3. These findings suggest that a high efficiency might be achieved with low G^{inject}t, low Greg, small total, and high V_{OC}. Due to S4's beneficial performance in terms of the parameters mentioned above, as shown by our theoretical results, the performance of DSSCs sensitized with it may be better than when utilizing other dyes.

5 Absorption spectra

Acetonitrile solvent examines how the terminal electron donor affects the described dyes' absorption characteristics. Figures 5 and 6 show the absorption spectra, while Tables 3 and 4 in the gas and solvent phases exhibit essential statistics. When calculating the absorption at the B3LYP level, all the dyes show two separate absorption bands, one in the 400–470 nm and another in the 500–670 nm region.The first band can be attributed to the HOMO-2 to LUMO - 1 transition, whereas the second band is associated with intramolecular charge transfer (ICT) via the HOMO to LUMO transition. Therefore, we draw novel conclusions based on an absorption maximum in the 400–470 nm region attributed to intramolecular charge transfer or an electron jumping from the HOMO orbital to the LUMO orbital.

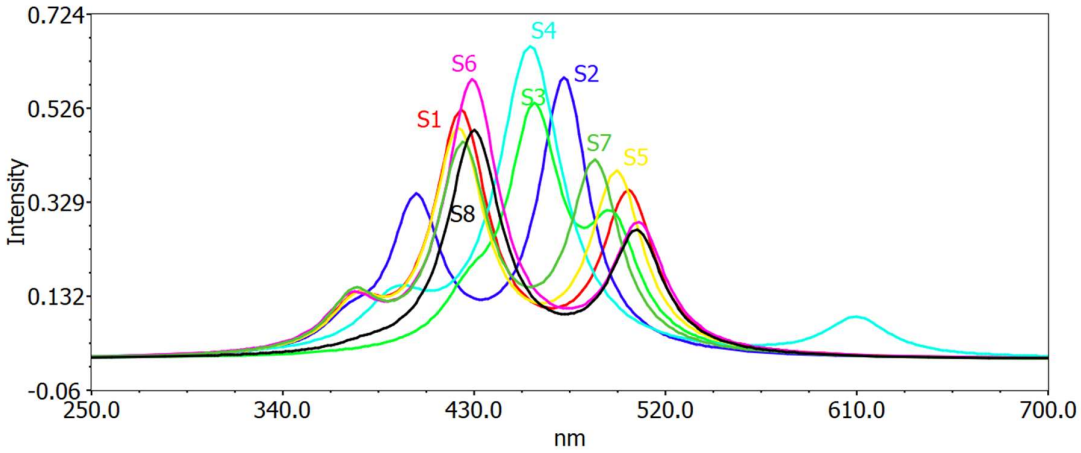

Figure 5: Calculated UV absorption spectra of the molecules calculated by TD/DFT/B3LYP/6-311G++ level in the gas phase.

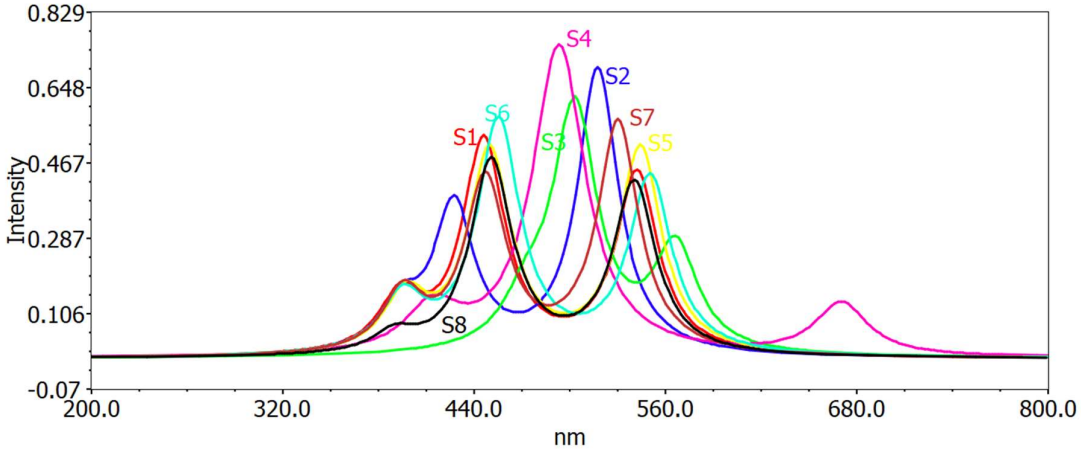

Figure 6: Calculated UV absorption spectra of the molecules calculated by TD/DFT/B3LYP/6-311G++ level in the solvent phase.

Table 3 Electronic transition data of the donor monomer molecules obtained by TD-DFT/B3LYP/6-311G++ level calculations in gas (H=HOMO; L=LUMO).

Dye	transition	λmax(eV)	λmax(nm)	f	MO	Orbital Contributions%
1	S1	2.4656	502.85	0.3371	H ->L	1.88
	S2	2.9246	423.93	0.5049	H-2 ->L	3.60
					H-1 ->L	93.74
	S3	3.3112	374.44	0.0939	H-3 ->L	5.18
					H-2->L	87.27
					H-1 ->L	3.05
2	S1	2.6239	472.52	0.5784	H-1 ->L	3.12
					H ->L	95.90
	S2	3.0778	402.83	0.3165	H-2 ->L	3.95
					H-1 ->L	91.36
					H ->L	2.24
	S3	3.336	371.66	0.0551	H-3 ->L	2.79
					H-2 ->L	86.97
					H-1 ->L	2.74
3	S1	2.5022	495.5	0.241	H-1 ->L	2.27
					H ->L	94.71
					H ->140	2.16
	S2	2.705	458.35	0.4886	H-1 ->L	4.68
					H ->140	91.89
	S3	2.8971	427.97	0.0872	H-4 ->L	6.23
					H-3 ->L	13.03
					H-2 ->L+1	2.79
					H-2 ->L	53.02
					H-1 ->L+1	14.37
					H ->L	2.22
4	S1	2.0316	610.29	0.0805	131 ->132	99.75
	S2	2.7156	456.57	0.6492	130 ->132	96.45
	S3	3.154	393.43	0.1034	128 ->132	10.61
					129 ->132	85.50
5	S1	2.4933	497.27	0.3769	H ->L	97.38
	S2	2.9322	422.83	0.463	H-1 ->L	3.52
					H-3 ->L	93.81
	S3	3.3073	374.88	0.0949	H-5 ->L	4.49
					H-3 ->L	4.10
					H-2 ->L	84.32
					H-1 ->L	3.04
6	S1	2.4424	507.64	0.2671	H-2 ->L	98.35
	S2	2.8881	429.3	0.5725	H-2 ->L	2.13
					H-1 ->L	95.55
	S3	3.3276	372.6	0.0998	H-5 ->L	4.77
					H-3 ->L	19.11
					H-2 ->L	69.62

					H-1 ->L	2.13
7	S1	2.5458	487.02	0.3955	H-1 ->L	2.19
					H ->L	96.84
	S2	2.9186	424.81	0.4285	H-1 ->L	94.53
	S3	3.3176	373.72	0.1118	H-5 ->L	3.24
					H-3 ->L	15.16
					H-2 ->L	74.54
					H-1 ->L	2.03
8	S1	2.4464	506.81	0.2546	H-2 ->L	2.46
					H-1 ->L	96.63
	S2	2.8822	430.17	0.4712	H-4 ->L	3.68
					H-3 ->L	2.41
					H-2 ->L	91.15
	S3	3.276	378.46	0.0103	H-5 ->L	2.59
					H-4 ->L	44.54
					H-3 ->L	50.41

Table 3 Electronic transition data of the donor monomer molecules obtained by TD-DFT/B3LYP/6-311G++ level calculations in solvent (H=HOMO;L=LUMO).

Dye	transition	λmax(eV)	λmax(nm)	f	MO	Orbital Contributions%
1	S1	2.2858	542.40	0.4367	H ->L	99.39
	S2	2.7782	446.28	0.5114	H-1->L	96.86
	S3	3.1458	394.12	0.1322	H-4 ->L	4.20
					H-2 ->L	91.85
	S3	5.0973	243.24	0.0478	H ->L+2	5.32
					H-1 ->L+4	6.39
					H-2 ->L+3	11.02
					H-2 ->L+1	2.02
					H-3 ->L+2	4.44
					H-3 ->L+5	11.51
					H-4 ->L+3	35.15
2	S1	2.3939	517.9100	0.6874	H ->L	98.41
	S2	2.8993	427.63	0.3524	H-1 ->L	4.08
					H-2 ->L	93.83
	S3	3.146	394.11	0.1065	H-2 ->L	2.11
					H-2 ->L	90.62
					H-1 ->L	3.66
3	S1	2.1881	566.62	0.2511	H ->L	97.26
	S2	2.4634	503.31	0.5883	H-1 ->L	3.66
					H-1	94.25
	S3	2.6214	472.97	0.0983	H-1 ->L	2.23
					H-1 ->L	13.73
					H-2 ->L	73.99
					H-1 ->L+1	2.53

					H->L+1	3.74
4	S1	1.8488	670.62	0.1267	H ->L	99.82
	S2	2.5126	493.44	0.7457	H-1 ->L	98.39
	S3	2.9921	414.37	0.1086	H-3 ->L	13.50
					H-2 ->L	84.31
5	S1	2.2773	544.43	0.4974	H ->L	99.18
	S2	2.7559	449.89	0.4864	H-2 ->L	2.52
					H-1 ->L	96.25
	S3	3.1216	397.19	0.1366	H-5 ->L	2.51
					H-3->L	2.66
					H-2 ->L	89.69
					H-1->L	2.59
6	S1	2.2513	550.72	0.4266	H ->L	99.35
	S2	2.7214	455.59	0.5585	H-1 ->L	97.29
	S3	3.1245	395.55	0.1337	H-3 ->L	10.24
					H-2 ->L	82.71
7	S1	2.3367	530.60	0.5583	H ->L	99.00
	S2	2.7709	447.45	0.4160	H ->L	96.83
	S3	3.1341	395.59	0.1435	H ->L	15.94
					H-1 ->L	76.91
8	S1	2.2925	540.82	0.4133	H ->L	98.72
	S2	2.7491	450.99	0.4661	H-2 ->L	2.31
					H-1 ->L	94.81
	S3	3.1742	390.61	0.0466	H-3 ->L	93.02
					H-1 ->L	2.09

The band wavelengths of the ICT transition of the studied dyes are classified in the following order: D2 (432.06) < D1 (433.26) < D4 (441.40) < D3 (442.62) < D5 (447.78). Dyes D1 and D2 show almost comparable values of λmax, while D3, D4, and D5, with the longest terminalelectron donors, present a small red-shift compared with D1.

The band wavelengths of the ICT transition of the studied dyes are classified in the following order: D2 (432.06) < D1 (433.26) < D4 (441.40) < D3 (442.62) < D5 (447.78). Dyes D1 and D2 show almost comparable values of λ_{max}, while D3, D4, and D5, with the most extended terminalelectron donors, present a small red-shift compared with D1.D4 exhibits the highest red-shift compared to the other dyes, which can be explained by the additional carbazole molecule's strong induction of a terminal electron donor, as opposed to the weaker dyes. Comparing S1,S5, S7, S8, and S2, S3,S6, and S4 with the thiophane group reveals that these groups are present, which can be attributed to the effects of the carbazole donor acting as an electron donor.

4 Conclusions

To create high-performance dyes for DSSCs, we examined several carbazole-based dyes with various terminal electron donors. The border molecular orbitals of all the investigated dyes are calculated, and their geometrical, electronic structure, optical absorption, and transition features are described. To find sensitizers with potential for use in DSSCs, the role of the

various terminal electron donors in regulating the geometry, electronic structure, and optical properties is evaluated based on the computational results, and the various parameters affecting V_{OC} and J_{SC} are discussed.The findings demonstrate that these dyes, particularly D4 with indole as the terminal electron donor, display good optoelectronic properties for application in DSSCs. Furthermore, due to its narrow energy gap, superior optical qualities, acceptable FMO energy levels, lowest total value, and greater G^{inject} and G^{Reg} values compared to the other tested dyes, the latter is discovered to be the best photosensitizer. As a result, a DSSC sensitized with S4 dye may have good optoelectronic characteristics compared to other dyes, increasing the overall efficiency of energy conversion.

References

[1]. Abas N, Kalair A, Khan N. Review of fossil fuels and future energy technologies. *Futures*. 2015;69:31-49.

[2]. Robertson N. Optimizing dyes for dye-sensitized solar cells. *Angew Chem Int Ed Engl*. 2006;45(15):2338-2345.

[3]. Tibebu S, Hailu A. Design, construction, and evaluation of the performance of dual-axis Sun trucker parabolic solar cooker and comparison of cooker. *J Renew Energy*. 2021;2021:8944722. doi:Crossref.

[4]. Owusu PA, Sarkodie SA. A review of renewable energy sources, sustainability issues and climate change mitigation. *Cog Eng*. 2016;3:1167990. doi:Crossref.

[5]. Usman Z, Tah J, Abanda H, Nche C. A critical appraisal of pv-systems' performance. *Buildings*. 2020;10:192. doi:Crossref.

[6]. Luceño-Sánchez JA, Díez-Pascual AM, Peña Capilla R. Materials for photovoltaics: state of art and recent developments. *Int J Mol Sci*. 2019;20(4):976.

[7]. Grätzel M. Photoelectrochemical cells. *Nature*. 2001;414(6861):338-344.

[8]. Hagfeldt A, Boschloo G, Sun L, Kloo L, Pettersson H. Dyesensitized solar cells. *Chem Rev*. 2010;110(11):6595-6663.

[9]. Gonçalves LM, de Zea Bermudez V, Ribeiro HA, Mendes AM. Dye-sensitized solar cells: a safe bet for the future. *Energy Environ Sci*. 2008;1(6):655-667.

[10]. O'Regan B, Grätzel M. A low-cost, high-efficiency solar cell based on dye-sensitized colloidal TiO2 films. *Nature*. 1991;353(6346):737-740.

[11]. Chen CY, Wang M, Li JY, et al. Highly efficient light-harvesting ruthenium sensitizer for thin-film dye-sensitized solar cells. *ACS Nano*. 2009;3(10):3103-3109.

[12]. Mishra A, Fischer MKR, Bäuerle P. Metal-free organic dyes for dye-sensitized solar cells: from structure: property relationships to design rules. *Angew Chem Int Ed Engl*. 2009;48(14):2474-2499.

[13]. Kuang D, Walter P, Nüesch F, et al. Co-sensitization of organic dyes for efficient ionic liquid electrolyte-based dye-sensitized solar cells. *Langmuir*. 2007;23(22):10906-10909.

[14]. Qin P, Yang X, Chen R, et al. Influence of π-conjugation units in organic dyes for dye-sensitized solar cells. *J Phys Chem C*. 2007;111:1853-1860.

[15]. Mathew S, Yella A, Gao P, et al. Dye-sensitized solar cells with 13% efficiency achieved through the molecular engineering of porphyrin sensitizers. *Nat Chem*. 2014;6(3):242-247.

[16]. Cai S, Tian G, Li X, Su J, Tian H. Efficient and stable DSSc sensitizers based on substituted dihydroindolo [2, 3-b] carbazole donors with high molar extinction coefficients. *J Mater Chem A*. 2013;1:11295-11305.

[17]. Koumura N, Wang ZS, Mori S, Miyashita M, Suzuki E, Hara K. Alkyl-functionalized organic dyes for efficient molecular photovoltaics. *J Am Chem Soc*. 2006;128(44):14256-14257.
[18]. Hwang S, Lee JH, Park C, et al. A highly efficient organic sensitizer for dye-sensitized solar cells. *Chem Commun (Camb)*. 2007;46(46):4887-4889.
[19]. Liang M, Chen J. Arylamine organic dyes for dye-sensitized solar cells. *Chem Soc Rev*. 2013;42(8):3453-3488.
[20]. Cai L, Moehl T, Moon SJ, et al.: 4. 9-dihydro-4, 4, 9, 9-tetrahexyl-s-indaceno (1, 2-b: 5, 6-b'). *Org Lett*. 2014;16(1):106-109.
[21]. Liu J, Yang X, Islam A, et al. Efficient metal-free sensitizers bearing circle chain embracing π-spacers for dye-sensitized solar cells. *J Mater Chem A*. 2013;1:10889-10897.
[22]. Kim JY, Kim YH, Kim YS. Indoline dyes with various acceptors for dye-sensitized solar cells. *CurrAppl Phys*. 2011;11(1):S117-S121
[23]. Liu B, Wu W, Li X, et al. Molecular engineering and theoretical investigation of organic sensitizers based on indoline dyes for quasi-solid state dye-sensitized solar cells. *Phys Chem Chem Phys*. 2011;13(19):8985-8992.
[24]. Liu B, Li W, Wang B, et al. Influence of different anchoring groups in indoline dyes for dyesensitized solar cells: electron injection, impedance and charge recombination. *J Power Sources*. 2013;234:139-146.
[25]. Cho MJ, Park SS, Yang YS, Kim JH, Choi DH. Molecular design of donor–acceptor-type cruciform dyes for efficient dyes-sensitized solar cells. *Synth Met*. 2010;160:1754-1760.
[26]. Ding W-L, Wang D-M, Geng Z-Y, Zhao X-L, Xu W-B. Density functional theory characterization and verification of high-performance indoline dyes with D–A–π–A architecture for dye-sensitized solar cells. *Dyes Pigments*. 2013;98:125-135.
[27]. Zhao Z, Xu X, Wang H, Lu P, Yu G, Liu Y. Zigzag molecules from pyrene-modified carbazole oligomers: synthesis, characterization, and application in OLEDs. *J Org Chem*. 2008;73(2):594-602.
[28]. Li T, Gao J, Cui Y, Zhong C, Ye Q, Han L. Novel D–π–A carbazole sensitizers with 4-phenyl-2-(thiophen-2-yl) thiazole as π-bridge for dye-sensitized solar cells. *J PhotochemPhotobiol A*. 2015;303-304:91-98.
[29]. Liu D, Fessenden RW, Hug GL, Kamat PV. Dye capped semiconductor nanoclusters. Role of back electron transfer in the photosensitization of SnO2 nanocrystallites with cresyl violet aggregates. *J Phys Chem B*. 1997;101:2583-2590.
[30]. Gaussian09, R.A.: 1, Frisch MJ, Trucks GW, Schlegel HB, et al. *Gaussian. Inc., Wallingford CT* 2009.
[31]. Becke AD. Density-functional thermochemistry. III. The role of exact exchange. *J Chem Phys*. 1993;98(7):5648-5652.
[32]. Krishnan R, Binkley JS, Seeger R, Pople JA. Self-consistent molecular orbital methods. XX. A basis set for correlated wave functions. *J Chem Phys*. 1980;72:650-654.
[33]. Fahim ZME, Bouzzine SM, Youssef AA, Bouachrine M, Hamidi M. Ground state geometries, UV/vis absorption spectra and charge transfer properties of triphenylamine–thiophenes based dyes for DSSCs: a TD-DFT benchmark study. *ComputTheor Chem*. 2018;1125:39-48.

[34]. Becke AD. A new mixing of Hartree-Fock and local densityfunctional theories. *J Chem Phys*. 1993;98:1372-1377.
[35]. Barone V, Cossi M. Quantum calculation of molecular energies and energy gradients in solution by a conductor solvent model. *J Phys Chem A*. 1998;102(11):1995-2001.
[36]. Cossi M, Rega N, Scalmani G, Barone V. Energies, structures, and electronic properties of molecules in solution with the C-PCM solvation model. *J Comput Chem*. 2003;24(6):669-681.
[37]. Frisch A, Nielsen AB, Holder AJ. *GaussView User Manual*. Gaussian Incorp; 2000:556.
[38]. Allouche AR. *Gabedit*; 2017.
[39]. El Mzioui S, Bouzzine SM, Bouachrine M, Bennan MN, Hamidi M. Effect of the alkyl chain length incorporated into donor part on the optoelectronic properties of the carbazole based dyes: theoretical study. Orbital. 2017.
[40]. Khan SU-D, Mahmood A, Rana UA, Haider S. Utilization of electron-deficient thiadiazole derivatives as π-spacer for the red shifting of absorption maxima of diarylamine–fluorene based dyes. *Theor Chem Acc*. 2015;134:1596.
[41]. Liu J, Sun X, Li Z, et al. New D–π–A system dye based on dithienosilole and carbazole: synthesis, photo-electrochemical properties and dyesensitized solar cell performance. *J PhotochemPhotobiol A*. 2014;294:54-61.
[42]. Huang J-F, Liu J-M, Tan L-L, et al. Novel carbazole based sensitizers for efficient dye-sensitized solar cells: role of the hexyl chain. *Dyes Pigments*. 2015;114:18-23.
[43]. Narayan MR. Dye sensitized solar cells based on natural photosensitizers. *Renew Sustain Energy Rev*. 2012;16:208-215.
[44]. Hamann TW, Jensen RA, Martinson ABF, Van Ryswyk H, Hupp JT. Advancing beyond current generation dye-sensitized solar cells. *Energy Environ Sci*. 2008;1(1):66-78.
[45]. Wang J, Cong S, Wen S, Yan L, Su Z. A rational design for dye sensitizer: density functional theory study on the electronic absorption spectra of organoimido-substituted hexamolybdates. *J Phys Chem C*. 2013;117(5):2245-2251.
[46]. Wang J, Li H, Ma N-N, Yan L-K, Su Z-M. Theoretical studies on organoimido-substituted hexamolybdates dyes for dyesensitized solar cells (DSSc). *Dyes Pigments*. 2013;99(2):440-446.
[47]. Zhang J, Li H-B, Zhang J-Z, et al. A promising anchor group for efficient organic dye sensitized solar cells with iodine-free redox shuttles: a theoretical evaluation. *J Mater Chem A*. 2013;1(44):14000-14007.
[48]. Zhang Z-L, Zou L-Y, Ren A-M, Liu Y-F, Feng J-K, Sun C-C. Theoretical studies on the electronic structures and optical properties of star-shaped triazatruxene/heterofluorene copolymers. *Dyes Pigments*. 2013;96:349-363.
[49]. Mubashar U, Farhat A, Khera RA, Iqbal N, Saleem R, Iqbal J. Designingandtheoreticalstudyoffluorinatedsmallmolecule donor materials for organic solar cells. *J Mol Model*. 2021;27(7):216.
[50]. Mahmood A, Tahir MH, Irfan A, Al-Sehemi AG, Al-Assiri MS. Heterocyclic azo dyes for dye sensitized solar cells: a quantum chemical study. *ComputTheor Chem*. 2015;1066:94-99.
[51]. Sun LL, Zhang T, Wang J, Li H, Yan LK, Su ZM. Exploring the influence of electron donating/withdrawing groups on hexamolybdate-based derivatives for efficient p-type dye-sensitized solar cells (DSSCs). *RSC Adv*. 2015;5(50):39821-39827.

[52]. Zhang J, Li H-B, Sun S-L, Geng Y, Wu Y, Su Z-M. Density functional theory characterization and design of highperformance diarylamine–fluorene dyes with different π spacers for dye-sensitized solar cells. *J Mater Chem*. 2012;22(2):568-576.
[53]. Li M, Kou L, Diao L, et al. Theoretical study of WS-9-Based organic sensitizers for unusual vis/NIR absorption and highly efficient dye-sensitized solar cells. *J Phys Chem C*. 2015;119:9782-9790.
[54]. Afolabi SO, Semire B, Akiode OK, Afolabi TA, Adebayo GA, Idowu MA. Design and theoretical study of phenothiazine-based low bandgap dye derivatives as sensitizers in molecular photovoltaics. *Opt Quantum Electron*. 2020;52(11):476.